International Journal of Thermodynamics (IJoT)*(8 pt Arial Bold)*
ISSN 1301-9724 / e-ISSN 2146-1511
https://dergipark.org.tr/en/pub/ijot

Vol. 27 (No. 4), pp. 043-055, 2024
doi: 10.5541/ijot.1486368
Published online: December 1, 2024

Research Article

Highly Efficient Energy Integration: Thermodynamic Analysis of Heat Recovered from SOFC Through S-CO_2 And Kalina Cycles

[1]*A. Elbir

[1*]Suleyman Demirel University Renewable Energy Resources Research and Application Center
E-mail: [1]*ahmetelbir@sdu.edu.tr

Received 19 May 2024, Revised 28 Sep 2024, Accepted 14 Nov 2024

Abstract

This study focuses on the implementation of a highly efficient energy integration using solid oxide fuel cell (SOFC) technology. A detailed thermodynamic analysis of the integration of heat energy obtained from SOFC into the Supercritical Carbon Dioxide (S-CO_2) cycle and the Kalina cycle aims to assess its effectiveness, sustainability, and economic performance in energy systems. The study presents a thermodynamic analysis encompassing the integration of SOFC technology into an energy system, as well as the integration of the heat energy obtained into the S-CO_2 cycle, Kalina cycle, and hot water production. The high energy efficiencies, low carbon emissions, and economic advantages individually achieved by SOFC, S-CO_2 cycle, and Kalina cycle are significantly enhanced when integrated into a cohesive system. The integrated system analysis results show an energy efficiency of 89.1%, an exergy efficiency of 64.6%, and an exergetic sustainability index of 0.83, demonstrating that this integration provides an energy solution with high efficiency, sustainability, and a low carbon footprint. Thermodynamic analyses were performed using the EES (Engineering Equation Solver) software. The main contribution of this study is the introduction of innovative approaches to energy efficiency and exergy analysis. The system achieves high energy efficiency through the integration of SOFC and the Kalina cycle. Particularly, optimizing the thermal management of the SOFC and utilizing the ammonia-water mixture more efficiently in the Kalina cycle brings significant improvements in the system's energy and exergy efficiency. These analyses demonstrate higher efficiency and sustainability compared to existing systems, emphasizing the originality of this approach.

Keywords: *Solid oxide fuel cell; supercritical CO_2; kalina cycle; energy analysis; exergy analysis.*

1. Introduction

In research aimed at enhancing the efficiency and sustainability of modern energy systems, there is a growing emphasis on the high potential of heat recovered from solid oxide fuel cells (SOFC) in energy recycling. In this context, this study presents a thermodynamic analysis of a highly efficient energy integration strategy involving the integration of heat obtained from SOFC power sources into the Supercritical Carbon Dioxide (S-CO_2) cycle and the Kalina cycle, respectively. The analysis aims to contribute significantly to the field of sustainable energy production by thoroughly evaluating the system's performance in terms of energy and exergy.

Numerous studies in the field have proposed innovative Combined Cooling, Heating, and Power (CCHP) systems, all built upon the concept of energy cascading. Among these, a notable system, integrating SOFC/GT (Solid Oxide Fuel Cell/Gas Turbine) and trans-critical CO_2 power/cooling cycles, showcased impressive capabilities, delivering 48.37 kW of cooling, 240.65 kW of heating, and 250.95 kW of net electricity production, with power generation and exergetic efficiency levels reaching 62.65% and 62.27%, respectively [1]. In its configuration, the excess heat generated by the proton exchange membrane (PEM) fuel cells is designed to be efficiently recovered using an organic Rankine cycle (ORC) system, further supported by a liquefied natural gas (LNG) subsystem for efficient heat exchange within the ORC. A comprehensive exergo-environmental analysis was conducted to assess the ecological impacts of irreversible processes occurring in the system.In this proposed setup, PEM fuel cells serve as the primary power generation source. Outputs from both the ORC and LNG subsystems are used to develop a transcritical CO_2 compression refrigeration system and to provide a reverse osmosis desalination unit. This integrated approach enables the system to achieve a fresh water production rate of 6 kg/s along with 1214 kW of electricity, 1116 kW of cooling capacity and 161.1 kW of heating capacity [2]. Furthermore, a groundbreaking cogeneration system, combining a gas turbine cycle, a supercritical CO_2 cycle, and a Kalina cycle, has emerged for integrated heating and power generation purposes. Comprehensive energy, exergy, and exergoeconomic analyses have been conducted to assess the system's performance and feasibility. The study findings unveil remarkable energy and exergy efficiencies of 78.15% and 40.97%, respectively. Economic scrutiny under specific pricing conditions reveals a promising payback period of 6.9 years and a net present value of $5.374 million [3]. Additionally, a newly devised cogeneration setup effectively merges solid oxide fuel cell (SOFC), internal combustion

*Corresponding Author

engine (ICE), supercritical carbon dioxide (S-CO_2) power cycle, and heat recovery steam generators (HRSG). With a combined output power of 345.58 kW and a net output power of 288.94 kW, the system attains an economical unit cost of 42.98 $/GJ, coupled with theoretical and actual generation efficiencies of 48.00% and 40.13%, respectively. Noteworthy is the overall energy efficiency reaching 65.82%, complemented by an exergy efficiency of 42.28% [4]. This investigation unveils a system composed of a solid oxide fuel cell (SOFC), a solar tower facility, and a (S-CO_2) Brayton cycle. Through multi-objective optimization, it is demonstrated that integrating an additional simple S-CO_2 cycle and a re-compression S-CO_2 cycle leads to notable achievements, including an exergy efficiency of 56.86% and a total system economic ratio of 513.10 $/hour, with specific metrics of 56.45% for exergy efficiency and 481.59 $/hour for total system economic ratio [5]. Furthermore, the introduction of a biomass-based solid oxide fuel cell (SOFC)-supported poly-generation system marks a significant advancement. Integrating a transcritical CO_2 cycle, re-compression (S-CO_2) Brayton cycle, and a double-effect LiBr absorption refrigerator, the system attains exceptional performance metrics, boasting an overall efficiency of 93.00% and an exergy efficiency of 29.95%. Under optimal conditions, the system can generate a maximum net power of 99.66 kW when the SOFC inlet temperature is set at 550°C and the current density reaches 3680 A/m2 [6]. Moreover, in the proposed integrated system, waste heat from the SOFC is efficiently recovered through a Kalina cycle, enhancing overall efficiency. Additionally, simultaneous cooling and power supply functions are fulfilled by utilizing waste heat from the Kalina cycle for liquefied natural gas (LNG) cold flow. Results underscore the system's efficacy, achieving approximately 55% exergy efficiency and 60% energy efficiency at a current density of 550 A/m2 [7]. Implementing a Kalina cycle for waste heat recovery from the SOFC stack and employing a thermoelectric generator to harness heat emitted from the Kalina condenser, this system demonstrates notable energy and exergy efficiencies of 58% and 54%, respectively, under optimal conditions [8]. The study further explores the integration of an organic Rankine cycle (ORC) into a solid oxide fuel cell (SOFC)-gas turbine (GT) hybrid power system. R1233zd(E) is selected as the working fluid for the ORC, showcasing significant energy and exergy efficiencies of 55.67% and 53.55%, respectively, under specific conditions. Economic and environmental evaluations under design conditions reveal a total cost rate of $36.09 per hour, with CO_2 emissions (EMI) at 355.8 kg/MWh. Comparative thermodynamic analyses indicate an 11.72% increase in exergy efficiency in the SOFC-GT-ORC configuration compared to the hybrid SOFC-GT cycle, highlighting the superiority of the hybrid SOFC-GT-ORC system. Moreover, the study suggests the potential utilization of alternative ORC working fluids such as R123, R601a, and R245fa in future applications [9]. Furthermore, a hybrid PV-SOFC system is analyzed by integrating actual load profiles and solar/air data into the system model. The PV and SOFC subsystems achieve maximum power outputs of 70 kWe and 152 kWe, respectively. The SOFC subsystem demonstrates average net electrical and total efficiencies of 30.3% and 70.0%, with peak values reaching 37.5% and 75.6%. [10]. In this system configuration, a (SOFC), a miniature gas turbine (MGT), a (S-CO_2) Brayton cycle, and a lithium bromide absorption refrigerator are integrated. By efficiently capturing waste heat from the SOFC-MGT combination using the S-CO_2 Brayton cycle, surplus electricity is generated. The excess heat from the MGT's exhaust is utilized for household heating and, via a lithium bromide absorption refrigerator, for both heating and cooling purposes, achieving an energetic return efficiency of 70.49% and an electrical efficiency of 60.59% [11]. Additionally, a Combined Heat and Power (CHP) system employing an SOFC is introduced. The study investigates the influence of various factors such as cell temperature, pressure, fuel utilization coefficient, and system air-to-fuel ratio on the performance of the SOFC-CHP setup. Reforming, electrochemical, and thermal models are concurrently introduced and solved to attain precise outcomes. Graphs depicting power and heat generation, as well as cell voltage loss, are generated under diverse operational conditions. It is observed that cell power increases with rising temperature and pressure, with temperature exhibiting a more pronounced effect. Moreover, the overall efficiency of the SOFC-CHP system is estimated to be approximately 73%. Finally, the optimal air-to-fuel ratio and fuel utilization coefficient are determined to be 9.4 and 0.85, respectively [12]. Their research has facilitated the integration of biomass gasification with (SOFC) technology. The hydrogen produced is introduced into the biomass gasification-SOFC system, proposing two distinct configurations. In the first configuration, hydrogen is directed into the anode inlet to provide a hydrogen-rich fuel, while in the second proposed configuration, it is injected into the SOFC's afterburner to elevate the gas turbine inlet temperature. These configurations undergo a thorough assessment and comparison from thermodynamic, environmental, and economic perspectives. It is evident that injecting hydrogen into the anode demonstrates superior performance in the system. Under the optimal operation of this configuration, the exergy efficiency, CO_2 emissions, and electricity cost are determined to be 24.85%, 0.257 kg/kWh, and 0.0911 $/kWh, respectively [13]. The relationship between heat transfer rate and entropy generation for single pressure and dual pressure waste heat recovery boilers has been examined. It has been stated that entropy generation per heat transfer is less in dual pressure boilers than in single pressure boilers because the temperature difference of heat transfer is less in dual pressure boilers. The analyses have shown that larger boilers (dual pressure) are both more efficient in terms of heat transfer and have less entropy generation per heat transfer [14]. They used the Kalina cycle instead of conventional methods for waste heat recovery. A system was designed with the Kalina cycle instead of the Rankine cycle. The designed system achieved an estimated efficiency increase of approximately 30%. The net power obtained from the Kalina cycle was calculated to be around 550 kW, whereas for the Rankine cycle, this value was calculated to be 420 kW. They stated that the Kalina cycle resulted in an annual fuel savings of 610.18 tons and a thermal efficiency increase of 4.8% [15]. They examined superheated and saturated vapor ORCs. A parametric study was conducted using different organic fluids to determine the best operating conditions for the system and to evaluate the findings of conventional exergy-based analyses. Conventional exergy and exergoeconomic analyses were calculated [16]. A theoretical performance analysis based on the exergetic performance coefficient, coefficient of performance (COP), exergy efficiency, and exergy destruction ratio criteria was conducted for a multipurpose refrigeration system using different

refrigerants under serial and parallel operating conditions. The exergetic performance coefficient criterion was defined as the ratio of exergy output to the total exergy destruction rate (or loss rate of availability) [17].

The imperative to enhance energy system efficiency and ensure sustainability is escalating in contemporary times. Within this context, the spotlight on the latent potential of heat derived from solid oxide fuel cells (SOFC) for waste heat recovery and the imperative of leveraging energy resources more effectively is progressively intensifying. This study posits that the integration of heat sourced from SOFCs into (S-CO_2) and Kalina cycles holds promise for augmenting overall system efficiency. Such integration harbors the prospect of judiciously exploiting waste heat and curbing carbon emissions. In contrast to antecedent studies, the proposed energy integration methodology focalizes on amalgamating SOFC heat with S-CO_2 and Kalina cycles. The distinctive feature of this study lies in its provision of novel perspectives on energy efficiency and waste heat utilization, thereby bridging extant gaps in the literature. While drawing upon antecedent research on energy integration strategies and waste heat recovery, this study's novelty lies in furnishing a comprehensive thermodynamic analysis of the amalgamation of SOFC heat with S-CO_2 and Kalina cycles, thus addressing a lacuna in the existing literature. The selection of S-CO_2 and Kalina cycles stems from their inherent advantages, including high efficiency, scalability, and proficient waste heat utilization. Nonetheless, the drawbacks of these systems, such as technological intricacy and cost implications, warrant consideration. The antecedent studies referenced in the introduction play a pivotal role in elucidating the subject matter. This study's contribution is underscored by its augmentation of existing literature and revelation of the potential inherent in integrating SOFC heat with S-CO_2 and Kalina cycles.

The motivation of this study is to present new approaches to increase the efficiency of existing energy systems and minimize energy losses. It is aimed to optimize energy recovery using solid oxide fuel cell (SOFC) technology and integrated thermodynamic systems. The study aims to increase energy efficiency especially by integrating SOFC's waste heat into the Super Critical Carbon Dioxide (S-CO_2) cycle and Kalina cycle. With this approach, both energy saving is achieved and sustainability is targeted with low carbon emissions. The study offers significant innovations in energy systems by providing higher energy and exergy efficiency compared to existing systems.

2. Methodology

The Solid Oxide Fuel Cell (SOFC) operates under steady-state conditions, meaning the system is modeled to function in equilibrium. The pressure within the system remains constant. This assumption implies that pressure is maintained at a continuous value throughout the analysis. The operation of the SOFC is considered ideal, assuming a fuel utilization rate of 100%. Real-world losses and interactions are not taken into account. The mixture ratio of fuel and oxidant is assumed to be ideal, reflecting a stoichiometric reaction assumption. The SOFC operates within a constant thermal bath at a specific temperature. Variations in temperature are not considered. The temperatures of the exhaust gases are equal to the temperature of the SOFC cells, indicating the condition of the gases within the cells. All heat transfer occurs within the environmental temperature limits between the cells. Heat transfer between cells is constrained within the environmental temperature limits. The SOFC operates in a thermodynamically reversible state, with irreversible entropy changes. The electrochemical reaction occurring at the anode represents the chemical reactions at both the cathode and anode of the SOFC. These reactions depict the interaction of fuel and oxidant through electrochemical processes.Air consists of 21% oxygen and 79% nitrogen, with an ambient temperature of 25°C and 1 bar. Considering hydrogen's purity and performing calculations on a unit mass/time basis, the flow rate is determined as 1 kmol/s, a considerably high flow rate. The operating temperature of the SOFC is set at 1000°C. The temperature in all heat exchangers is calculated with a 0.7 efficiency ratio. The Higher Heating Value of Hydrogen (HHV_{H2}) is 285830 kJ/kmol [12]. [13]. [18].

2.1. Assumptions For Thermodynamic Analysis Of S-CO_2 Cycle And Kalina Cycle

The system exhibits stable and consistent performance, indicating that the operating conditions of the system are predetermined and continue steadily. Only pure substances are used in the system, allowing for the use of ideal conditions in analysis and calculations.Compression processes for the compressor and pump occur adiabatically, signifying minimal interaction of energy transfer with the external environment. Pressure drops in system components and heat transfer in the pipeline are ignored in the analysis, reducing complexity and indicating theoretical modeling. The dead state of the circulating fluids in all cycles is considered as standard conditions: 25°C temperature and 1 bar atmospheric pressure. The system demonstrates regular and stable performance, implying that system parameters are under control, and expected values are approached consistently. In the analysis, the gravitational potential energy and kinetic energy of the fluids in the system are neglected, assuming these energy types have negligible effects on the system's performance in practice.

2.2. Assumptions For Thermodynamic Analysis Of SOFC

SOFC is generally a type of fuel cell that produces electrical energy through an electrochemical reaction between a fuel (usually hydrogen or methane) and an oxidant (typically oxygen in the air). Electrochemical reactions take place at the anode and cathode electrodes of the SOFC. The electrochemical reactions occurring at the anode and cathode electrodes of the SOFC are defined as equations, such as Equation 1 [18]:

$$H_2 + 2.381\ x\ (0.21\ x\ O2 + 0.79\ x\ N_2) \Rightarrow H_2O + 1.881\ x\ N_2 + \dot{Q}_{fc} + \dot{W}_{fc} \quad (1)$$

Equation 1 represents the electrochemical reaction of a solid oxide fuel cell (SOFC). SOFC produces electrical energy through a reaction between a fuel, such as hydrogen, and a mixture of oxygen and nitrogen in the air. This reaction occurs in the electrochemical process at the anode of the SOFC. The terms in the equation are as follows: Hydrogen (H_2) is the fuel supplied to the anode of the SOFC; Oxygen (O_2) is the primary oxidizing agent in the air; Nitrogen (N_2) is an inert gas present in the air; Water (H_2O) is produced as a result of the reaction; $\dot{Q}_{fc}$ represents the heat flow from the

SOFC; $\dot{W}_{fc}$ represents the electrical energy generated by the SOFC.

The first law of thermodynamics can be written as Equation 2:

$$\dot{N}_{H2} \text{ x } h_{H2}|_{in} + \dot{N}_{O2} \text{ x } h_{O2}|_{in} + \dot{N}_{N2} \text{ x } h_{N2}|_{in} - \dot{N}_{H2O} \text{ x } h_{H2O}|_{out} - \dot{N}_{N2} \text{ x } h_{N2}|_{out} + \dot{Q}_{fc} + \dot{W}_{fc} = 0 \quad (2)$$

Equation 2 represents the energy balance of a solid oxide fuel cell (SOFC). In this equation, the sum of enthalpy values of the inflowing and outflowing streams to the SOFC equals the heat and electric energy generated by the SOFC. The terms in the equation include: the molar flow rate of hydrogen ($\dot{N}_{H2}$), the molar enthalpy of inflowing hydrogen ($h_{H2}|_{in}$), the molar flow rate of oxygen ($\dot{N}_{O2}$), the molar enthalpy of inflowing oxygen ($h_{O2}|_{in}$), the molar flow rate of nitrogen ($\dot{N}_{N2}$), the molar enthalpy of inflowing nitrogen ($h_{N2}|_{in}$), the molar flow rate of water ($\dot{N}_{H2O}$), the molar enthalpy of outflowing water ($h_{H2O}|_{out}$), the molar flow rate of outflowing nitrogen ($\dot{N}_{N2}$), and the molar enthalpy of outflowing nitrogen ($h_{N2}|_{out}$). Additionally, the terms representing the heat flow from the SOFC ($\dot{Q}_{fc}$) and the electric energy flow from the SOFC ($\dot{W}_{fc}$) are included in the equation.

The second law of thermodynamics can be expressed as Equation 3.

$$\dot{N}_{H2} \text{ x } s_{H2}|_{in} + \dot{N}_{O2} \text{ x } s_{O2}|_{in} + \dot{N}_{N2} \text{ x } s_{N2}|_{in} - \dot{N}_{H2O} \text{ x } s_{H2O}|_{out} - \dot{N}_{N2} \text{ x } s_{N2}|_{out} + \frac{\dot{Q}_{fc}}{T_{fc}} + \dot{S}_{fc} = 0 \quad (3)$$

Equation 3 represents the entropy balance of a solid oxide fuel cell (SOFC). In this equation, the sum of the entropies of the inflowing and outflowing streams to and from the SOFC is equal to the total entropy production from the SOFC ($\frac{\dot{Q}_{fc}}{T_{fc}}$) divided by the absolute temperature of the cell (T_{fc}) and the entropy production rate due to irreversibility ($-\dot{S}_{fc}$). The terms in the equation are as follows: the molar flow rate of hydrogen ($\dot{N}_{H2}$), the molar entropy of inflowing hydrogen ($s_{H2}|_{in}$), the molar flow rate of oxygen ($\dot{N}_{O2}$), the molar entropy of inflowing oxygen ($s_{O2}|_{in}$), the molar flow rate of nitrogen ($\dot{N}_{N2}$), the molar entropy of inflowing nitrogen ($s_{O2}|_{in}$), the molar flow rate of water vapor ($\dot{N}_{H2O}$), the molar entropy of outflowing water vapor ($s_{H2O}|_{out}$), the molar flow rate of nitrogen leaving the system ($\dot{N}_{N2}$), and the molar entropy of outflowing nitrogen ($s_{N2}|_{out}$). Additionally, the term representing the entropy production rate due to irreversibility ($-\dot{S}_{fc}$) is divided by the absolute temperature of the cell (T_{fc})).

Here, $\dot{N}$ is the molar flow rate, "h" is the specific molar enthalpy, "S" is the specific molar entropy, "Tfc" is the absolute temperature of the fuel cell, and $\dot{S}g$ is the entropy production rate due to irreversibility. In this context, hin represents the enthalpy per mole of H_2 transported, while sin and sout denote the amounts of reactant inlet and reaction product outlet, respectively, per mole of H_2 taken from the system by the exhaust. The variables sin and sout are analogous to hin and hout, respectively. All these variables can be determined by the following expressions Equations (4),(5),(6),(7):

$$h_{in} = (h_{H2} + 0.5 x h_{O2} + 1.881 x h_{N2})_{in} \quad (4)$$

$$h_{out} = (h_{H2O} + 1.881 x h_{N2})_{out} \quad (5)$$

$$s_{in} = (s_{H2} + 0.5 x s_{O2} + 1.881 x s_{N2})_{in} \quad (6)$$

$$s_{out} = (s_{H2O} + 1.881 x s_{N2})_{out} \quad (7)$$

If we assume an ideal, energy-neutral process, the entropy generation is zero. The ideal power of the cell Equation (8):

$$\dot{W}_{fc} = -\dot{N}_{H2} \text{ x } (\Delta h - T_{fc} \text{ x } \Delta s) \quad (8)$$

When $\Delta h = h$ out $- h$ in and $\Delta s =$ s out $-$ s in , the enthalpy and entropy changes for the fuel cell reaction, respectively.

Given that the Gibbs free energy is expressed as g = h – T x s, the equivalent for isothermal processes can be rewritten as equation (9):

$$\dot{W}_{fc} = \dot{N}_{H2} \text{ x}(gin - gout) = -\dot{N}_{H2} x \Delta_g \quad (9)$$

Note that the previous equation is valid under the condition that reactants and product flows are at the default operating temperature of the cell. In this study, as the cell does not operate isothermally (reactants are at a lower temperature than the cell), eq. (9) is not applicable, and eq. (8) has been used to calculate the ideal power of the SOFC.

When the ideal power is obtained, efficiency can be formulated as follows when the maximum possible Process is reversible Equation (10):

$$\eta_{fc} = \frac{\dot{W}_{fc}}{-\dot{N}_{H2} \text{ x } \Delta_h} = \frac{\Delta h - T \text{ x } \Delta s}{\Delta h} \quad (10)$$

Equation 10 represents the efficiency of a (SOFC), which is defined as the ratio of the work output ($\dot{W}_{fc}$) to the heat input ($-\dot{N}_{H2} \text{ x } \Delta_h$). This can also be expressed as the ratio of the change in enthalpy (Δh) minus the product of the temperature (T) and the change in entropy (Δs) to the change in enthalpy (Δh).

In the non-isothermal process examined in this study, where the temperature of reactants is lower than that of the products, and under certain conditions, the Δs term can be greater than zero. In this scenario, equation (9) would imply that the fuel cell system absorbs heat from the surroundings and converts it entirely into electrical energy, potentially achieving a fuel cell efficiency higher than unity. However, this scenario is not feasible; thus, operating at the claimed temperature of the cell is unattainable, and the outlet temperature of the products will be lower [19].

Finally, in this study, the Δh (enthalpy change) used in equations (9) and (10) is not based on the higher heating value or lower heating value of the fuel; instead, it is based on the actual enthalpy change for the fuel cell reaction.

Thermodynamic analyses for the S-CO_2 cycle and Kalina cycle:

For steady state in thermodynamic analysis. the basic mass balance equation can be given as follows Equation (11) [20]. [21]. [22];

$$\sum \dot{m}_{in} = \sum \dot{m}_{ex} \quad (11)$$

The mass flow rate is denoted by $\dot{m}$, where the 'in' and 'ex' indices signify the inlet and outlet states, respectively. Equation (12) represents the energy balance:

$$\dot{Q}_{in} + \dot{W}_{in} + \sum_{in} \dot{m}\left(h + \frac{V^2}{2} + gz\right) = \dot{Q}_{ex} + \dot{W}_{ex} + \sum_{ex} \dot{m}\left(h + \frac{V^2}{2} + gz\right) \quad (12)$$

At this point, $\dot{Q}$ denotes the heat transfer rate, while $\dot{W}$ represents power. Specific enthalpy is denoted by h, velocity by v, height by z, and gravitational acceleration by g. Equation (13) expresses the entropy balance equation under steady-state conditions:

$$\sum_{in} \dot{m}_{in} s_{in} + \sum_{k} \frac{\dot{Q}}{T_k} + \dot{S}_{gen} = \sum_{ex} \dot{m}_{ex} s_{ex} \quad (13)$$

Here, s represents the specific entropy, and $\dot{S}_{gen}$ denotes the entropy generation rate. Equation (14) presents the exergy balance equation.

$$\sum \dot{m}_{in}\, ex_{in} + \sum \dot{E}\, x_{Q.in} + \sum \dot{E}x_{W.in} = \sum \dot{m}_{ex} ex_{ex} + \sum \dot{E}x_{Q.ex} + \sum \dot{E}x_{W.ex} + \dot{E}x_{D} \quad (14)$$

Equation 14, known as the exergy balance equation, expresses the conservation of exergy within a system. On the left side of the equation, incoming exergy flows are summed. These flows include the exergy values of the substances entering the system ($\sum \dot{m}_{in}\, ex_{in}$), the exergy associated with incoming heat transfer ($\sum \dot{E}\, x_{Q.in}$), and the exergy associated with incoming work transfer ($\sum \dot{E}x_{W.in}$). On the right side of the equation, outgoing exergy flows are summed. These flows include the exergy values of the substances leaving the system ($\sum \dot{m}_{ex} ex_{ex}$), the exergy associated with outgoing heat transfer ($\sum \dot{E}x_{Q.ex}$), and the exergy associated with outgoing work transfer ($\sum \dot{E}x_{W.ex}$). Additionally, the equation includes the exergy related to the work transfer applied externally to the system ($\dot{E}x_D$).

The specific flow exergy can be written as Equation (15):

$$ex = ex_{ph} + ex_{ch} + ex_{pt} + ex_{kn} \quad (15)$$

The kinetic and potential components of exergy are considered negligible. Additionally, the chemical exergy is assumed to be insignificant. The physical or flow exergy (ex_{ph}) is defined by Equation (16):

$$ex_{ph} = (h - h_o) - T_o(s - s_o) \quad (16)$$

In this context, h and s denote specific enthalpy and entropy, respectively. In real scenarios, h_o and s_o refer to enthalpy and entropy at reference medium states, respectively.

Exergy destruction is calculated as the product of specific exergy and mass, as expressed in Equation (17):

$$\dot{E}x_D = ex * m \quad (17)$$

The exergy ratios related to work, denoted as $\dot{E}x_D$, are provided by Equation (18):

$$\dot{E}x_D = T_0 \dot{S}_{gen} \quad (18)$$

The exergy ratios related to work, denoted as $\dot{E}x_W$, are provided by Equation (19):

$$\dot{E}x_W = \dot{W} \quad (19)$$

$\dot{E}x_Q$. are the exergy rates related to heat transfer and are given as below Equation (20).

The exergy rates related to heat transfer, denoted as $\dot{E}x_Q$, are given by Equation (20) below.

$$\dot{E}x_Q = \left(1 - \frac{T_o}{T}\right)\dot{Q} \quad (20)$$

Exergy destruction within the system Equation (21);

$$\dot{E}x_{D.syst.} = \dot{E}x_{in} - \dot{E}x_{aut} \quad (21)$$

What work comes out of the system Equation (22);

$$\dot{W}net_{out} = \dot{Q}_{in} - \dot{Q}_{out} \quad (22)$$

System thermal efficiency (η) Equation (23);

$$\eta = \frac{\text{energy in exit outputs}}{\text{total energy inlets}} \quad (23)$$

The exergy efficiency (ψ) can be defined as follows Equation (24);

$$\psi = \frac{\text{exergy in exit outputs}}{\text{total exergy inlets}} \quad (24)$$

2.3. Exergoenvironmental Analysis For Integrated System

Shows exergoenvironmental impact factor. $\dot{E}x_{D.tot.}$ is total exergy destruction rate. $\dot{E}x_{D.in.}$ is input exergy rate Equation (25) [23].

fei represents the exergoenvironmental impact factor $\dot{E}x_{D.tot.}$, denotes the total exergy destruction rate, while $\dot{E}x_{D.in.}$, represents the input exergy rate, as described in Equation (25) [23]

$$fei = \frac{\dot{E}x_{D.tot.}}{\dot{E}x_{D.in.}} \quad (25)$$

Cei is exergoenvironmental impact coefficient. ψ_{ex} represents exergy efficiency of the system Equation (26):

$$Cei = \frac{1}{\psi_{ex}/_{100}} \quad (26)$$

Φei represents the exergoenvironmental impact index, as defined in Equation (27).

$$\Phi ei = fei \times Cei \quad (27)$$

Φeii represents the improvement in exergoenvironmental impact, as described in Equation (28).

$$\Phi eii = \frac{1}{\Phi ei} \quad (28)$$

fes is the exergy stability factor, defined by Equation (29).

$$fes = \frac{\dot{E}x_{D.out.}}{\dot{E}x_{D.out.} + \dot{E}x_{D.tot.}} \quad (29)$$

Φest represents exergetic sustainability index Equation (30).

$$\Phi est = fes \times \Phi eii \quad (30)$$

To evaluate the carbon emissions stemming from electricity consumption, the formula [24] multiplies the direct energy consumption denoted as "E" by the carbon intensity factor "eCO_2". In this context, "E" represents the emissions quantity derived by subtracting the net power of the subcycle from the overall net power Equation (31):

$$\text{Carbon Emissions} = E \times eCO_2 \quad (31)$$

Countries can be categorized based on the carbon intensity of electricity generation, with three primary groups: Group A, exhibiting a carbon intensity of up to 0.29 kg.CO_2/kWh; Group B, ranging between 0.30 and 0.69 kg.CO_2/kWh; and Group C, exceeding 0.70 kg.CO_2/kWh [25].

The reduction in integrated system power production cost is determined by subtracting the net power gained from waste heat from the initially obtained net power, dividing this result by the system efficiency, and then multiplying it by the designated electricity price for cost assessment Equation (32):

$$\text{electricitycost} = \frac{\text{Power gained}}{\text{cycle efficiency}} * \text{electricityprice} \quad (32)$$

Electricity Cost represents the economic aspect of electricity per unit. Power Gained denotes the energy acquired by the system. Cycle Efficiency signifies the efficiency of the energy conversion cycle. With a carbon intensity of 0.50 kg.CO_2/kWh [25] and a unit electricity price of 0.14 $/kWh [26].

This equation provides a metric for understanding the economic implications of electricity generation per unit, considering the energy obtained, the efficiency of the energy conversion cycle, and the specific carbon intensity and unit electricity price values used in the calculation.

2.4. Overview Of The System

The diagram in Figure 1 illustrates the integrated power generation facility, which underwent thermodynamic analysis.

The system utilizes hydrogen (H_2) as the primary fuel. Hydrogen is directed from the storage tank to (SOFC) system through a heat exchanger-I. The pure hydrogen (The phrase 'facilitating a more rapid transformation' implies that the controlled introduction of pure hydrogen into the anode of the SOFC during its initial stages helps accelerate the conversion process. In other words, this controlled manner of introducing hydrogen at the beginning of the operation of the SOFC aids in speeding up the chemical reactions taking place within the fuel cell, resulting in a quicker onset of electricity generation.) is introduced to the anode of the SOFC in a controlled manner during its initial stages, facilitating a more rapid transformation. The oxidant employed in the system is a gas containing air. The air is heated through a separate heat exchanger-II. Subsequently, the preheated air is directed to the cathode of the SOFC. At the cathode, a reaction between oxygen and oxygen occurs, releasing electrons. The electrochemical outcomes at the anode and cathode involve the conversion of the chemical energy of hydrogen and oxygen into electrical energy and heat. These released electrons flow through the circuit, generating electrical energy [18].

The waste heat from the SOFC is initially transferred to a S-CO_2) cycle. Compressed CO_2 is directed to the heat absorption system, utilizing the high-temperature waste heat from the SOFC. At this stage, the waste heat from the SOFC expands the supercritical CO_2 by adding heat to it. The supercritical CO_2, now carrying the absorbed heat, expands through a turbine, producing energy. After electricity generation, the CO_2 gas is cooled and prepared for compression again to ensure the continuity and readiness for reuse. These steps enable the efficient utilization of waste heat in the supercritical carbon dioxide cycle. By converting waste heat into electrical energy, this system can enhance overall energy efficiency [18].

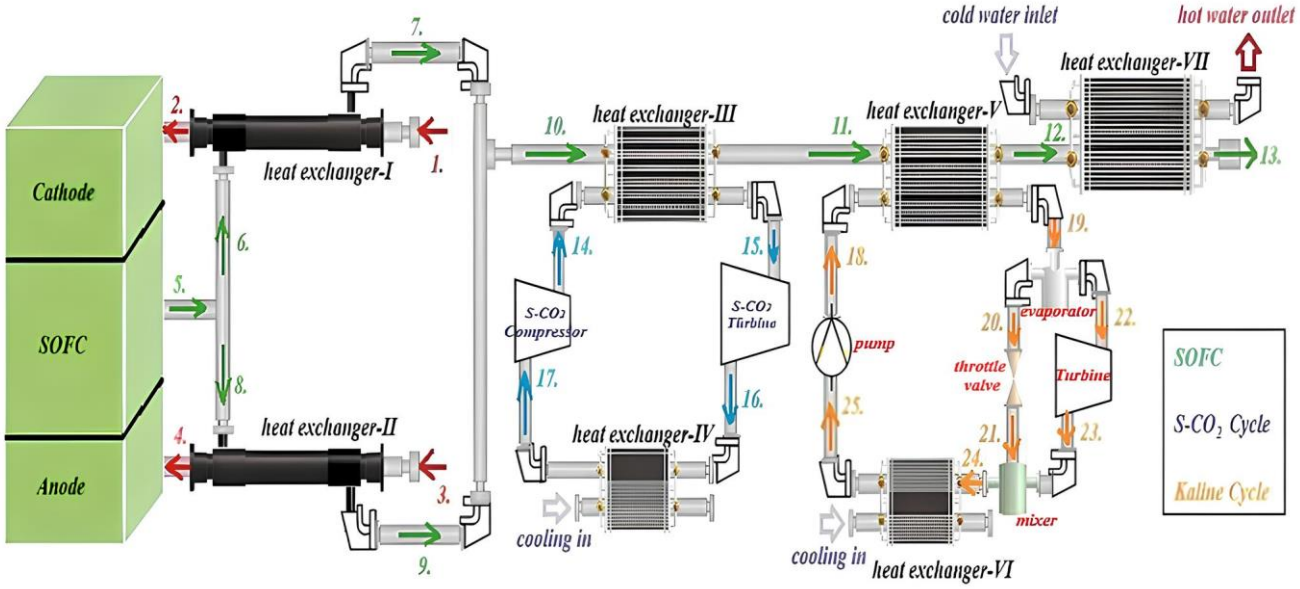

Figure 1. Integrated power generation facility with thermodynamic analysis.

In the second stage of waste heat from the SOFC, it is transferred to the heat exchanger-V containing a Kalina solution. The waste heat causes the solution to evaporate, triggering the evaporation reaction within the solution due to its low temperature. The evaporated solution expands through a turbine, producing electrical energy. The spent solution is condensed in a condenser. Additionally, a partition valve releases the high-pressure solution into a low-pressure region, ensuring pressure balance. This allows for the release and separation of vapor within the solution. The condensed solution is redirected to the heat exchanger, initiating a cycle. The heat generated during the condensation of the solution is returned to the heat exchanger to reuse the waste heat from the SOFC, constituting a heat recovery step that enhances the system's efficiency. The Kalina cycle is specifically designed for energy production from low-temperature heat sources, such as waste heat from SOFC. The evaporation and condensation within the solution, operating at low temperatures, increase the efficiency of the cycle. One of the advantages of this system is its applicability in various industrial processes and waste heat sources. Heat recovery aids in improving system efficiency, contributing to the reduction of overall energy consumption [19].

3. Findings And Discussion

3.1. Results For SOFC Analysis

Figure 2 shows the SOFC flowchart.

This Table 1 comprises the thermodynamic properties of different locations within (SOFC). Each location is characterized by specific temperature (T), molar flow rate ($\dot{N}$), composition, molar enthalpy (h), molar entropy (s), and exergy (Ex). It has been utilized to understand and optimize the behavior of SOFC under various operating conditions

Table 2 presents detailed results evaluating the performance of the Fuel Cell. The enthalpy change (Δh) during (SOFC) reactions is determined to be -215,452 kJ/kmol, and the entropy change (Δs) is -20.93 kJ/kmol.K. These thermodynamic parameters characterize the thermodynamic properties of SOFC in its energy production process. The electrical power ($\dot{W}_{fc}$) is measured at 188.81 kW, with a fuel cell energy efficiency (ηfc) of 87.63% and a fuel cell exergy efficiency (ψfc) of 61.33% calculated. These values indicate the high energy conversion efficiency of SOFC. The exergetic sustainability index is determined to be 0.70, reflecting the impact of exergy losses during SOFC's energy production on sustainability. While the system produces 94.4 kg of carbon emissions per hour, the economic value of the generated electricity is calculated at $34.42/hour. These results showcase that SOFC minimizes its environmental impact, offering an energy production process that is both sustainable and economically efficient. These findings underscore the significant role of SOFC in fuel cell technology, providing sustainable, efficient, and economically viable solutions for energy production.

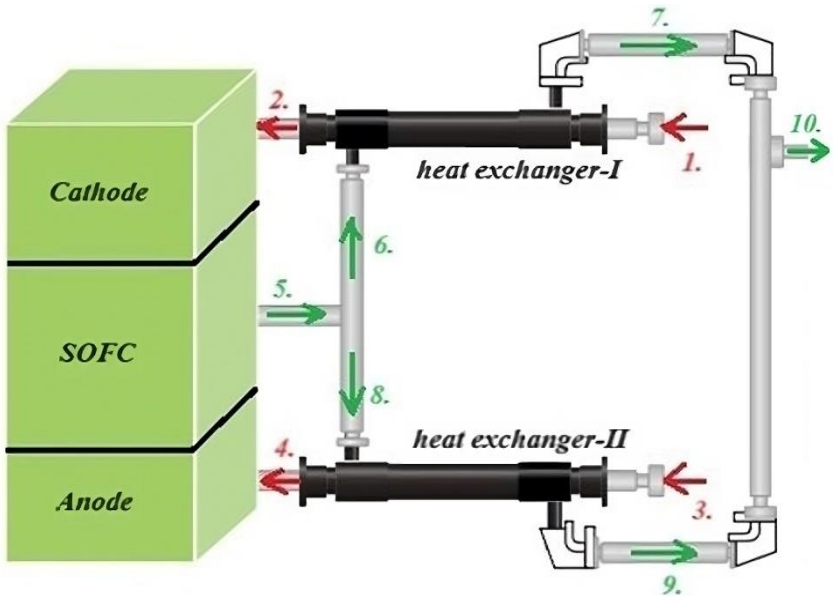

Figure 2. Flow chart of SOFC system.

Table 1. Thermodynamic properties of SOFC flow chart according to locations (T_0. dead state).

Location	T [°C]	h (kj/kmol)	$\dot{N}$ [mol/s]	Composition (mol%)		s [kj/kmolK]	Ex (Kw)
1.	25	0	1	CO:100		130.7	0
2.	694.7	19706	1	H_2:100		165.2	9.417
3.	25	0	2.381	O_2:21	N_2:79	198.7	0
4.	694.7	20665	2.381	O_2:21	N_2:79	244	23.736
5.	1000	-50866	2.881	H_2O:34.7	N_2:65.3	217.3	54.087
6.	1000	-50866	0.8239	H_2O:34.7	N_2:65.3	244	15.467
7.	317.5	-74785	0.8239	H_2O:34.7	N_2:65.3	217.3	2.301
8.	1000	-50866	2.057	H_2O:34.7	N_2:65.3	244	38.618
9.	317.5	-74785	2.057	H_2O:34.7	N_2:65.3	217.3	5.747
10.	317.5	-74785	2.881	H_2O:34.7	N_2:65.3	217.3	8.049
11.	190	-78833	2.881	H_2O:34.7	N_2:65.3	209.6	1.046
12.	85.51	-82076	2.881	H_2O:34.7	N_2:65.3	201.7	0.1678
13.	43.13	-83378	2.881	H_2O:34.7	N_2:65.3	197.8	0.01671
T0.	25	-83934		H_2O:34.7	N_2:65.3	162.2	

Table 2. Thermodynamic and calculations results for SOFC.

Parameters	values
Enthalpy change during fuel cell reactions (Δh)	-215452 (kJ/kmol)
Entropy change during fuel cell reactions (Δs)	-20.93 (kJ/kmol.K)
Electric power ($\dot{W}_{fc}$)	188.81kW
Fuel cell energy efficiency (ηfc)	% 87.63
Fuel cell exergy efficiency (ψfc)	% 61.33
exergetic sustainability index	0.70
Carbon emissions	94.4 kg/h
Economic value of the generated electricity	34.42 $/h

The technoeconomic analysis of the proposed system should be made more comprehensive by comparing it with similar plants in the existing literature. This comparison is an important step that will clearly demonstrate the economic feasibility of the proposed system.

Energy Production Costs: The energy production costs of the proposed system should be determined by analyzing the cost structure of each of the SOFC, S-CO_2 and Kalina cycles. In the existing literature, the energy production costs of similar plants generally vary between $ 50-70 per kWh. Comparing the costs in the proposed system with this range is important for evaluating the economic sustainability of the system.

Payback Periods: The payback periods of the proposed system should be calculated based on investment costs and annual revenues. The payback periods of similar systems in the existing literature generally vary between 5-8 years. Whether the payback period of the proposed system remains in this range will be an important indicator for investors.

Net Present Value (NPV): The net present value analysis will show the long-term economic performance of the proposed system. The NPV values of similar plants are generally positive and around $ 100,000. If the NPV value of the proposed system is above this value, it indicates that the system is attractive in terms of investment. This extended technoeconomic analysis will allow us to better understand the economic feasibility of the proposed system and increase its attractiveness to potential investors.

3.2. Results For S-CO_2 Analysis

Figure 3 gives the heat flow diagram of the supercritical carbon dioxide cycle.

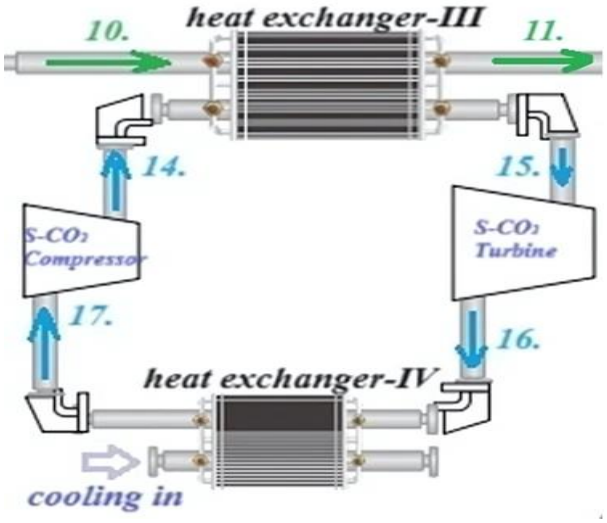

Figure 3. Flow chart of the S-CO_2 cycle.

Table 3. Thermodynamic data of the S-CO_2 cycle (T0. dead state).

Loc.	T [^{0}C]	s[kJ/kg.K]	P [bar]	h [kJ/kg]	ex [kj/kg]	m [kg/s]
14.	79.7	-1.075	140	-83.63	237.8	0.04629
15.	246.2	-0.4756	140	168.3	311.1	0.04629
16.	193.1	-0.4652	80	125	264.8	0.04629
17.	40	-1.08	80	-103.6	219.6	0.04629
T0.	25	0.00046	1	-0.883	0	-------

Table 3 presents the thermodynamic data of the S-CO_2 cycle. The table includes specific values of temperature (T), entropy (s), pressure (P), enthalpy (h), exergy (ex), and mass flow rate (m) at different locations. These data enable the analysis of the performance of the S-CO_2 cycle under various operating conditions.

Table 4. Results obtained within the of S-CO_2 cycle.

Parameters	Values
Electric power ($\dot{W}_{s-co2}$)	2 kW
S-CO_2 heat transfer rate with heat exchanger-III ($\dot{Q}_{s-CO2}$)	11.66 kW
S-CO_2 energy efficiency (ηs-CO_2)	% 15.9
S-CO_2 exergy efficiency (ψ s-CO_2)	% 47.2
exergetic sustainability index	0.37
Carbon emission	1 kg/h
Economic value of electricity	10.26 $/h

Table 4 presents the results for the Kalina cycle. The outcomes related to (S-CO_2) cycle are as follows: The electric power ($\dot{W}_{s-co2}$) is determined as 2 kW, signifying the electricity generated by the S-CO_2 cycle. The transferred heat through heat exchanger-III ($\dot{Q}_{s-CO2}$) is 11.66 kW, representing the heat transfer within the system. The S-CO_2 energy efficiency (η S-CO_2) is calculated as 15.9%, illustrating the energy conversion efficiency of the S-CO_2 cycle. The S-CO_2 exergy efficiency (ψ S-CO_2) is 47.2%, showcasing how effectively S-$_{CO2}$ minimizes energy losses. The Exergetic Sustainability Index value is 0.37, reflecting the relationship between the system's energy efficiency and sustainability. Carbon emissions are 1 kg/h, providing a measure of the carbon emissions produced by the system. The economic value of electricity is determined as 10.26 $/hour, expressing the economic viability of the electricity generated by the S-CO_2 cycle. These results encompass crucial parameters used to evaluate the performance and environmental impacts of the S-CO_2 cycle in the energy production process, indicating its potential to play an effective role in the energy sector.

3.3. Result For Kalina Cycle Analysis

Figure 4 shows the flow chart of the kalina cycle.

Table 5 provides the thermodynamic properties of the cycle. It includes data such as temperature (T), enthalpy (h), entropy (s), pressure (P), exergy (ex), mass flow rate (m), ammonia concentration (%NH_3), and the fluid used at different locations within the cycle. These properties are essential for analyzing the performance and behavior of the cycle under various operating conditions.

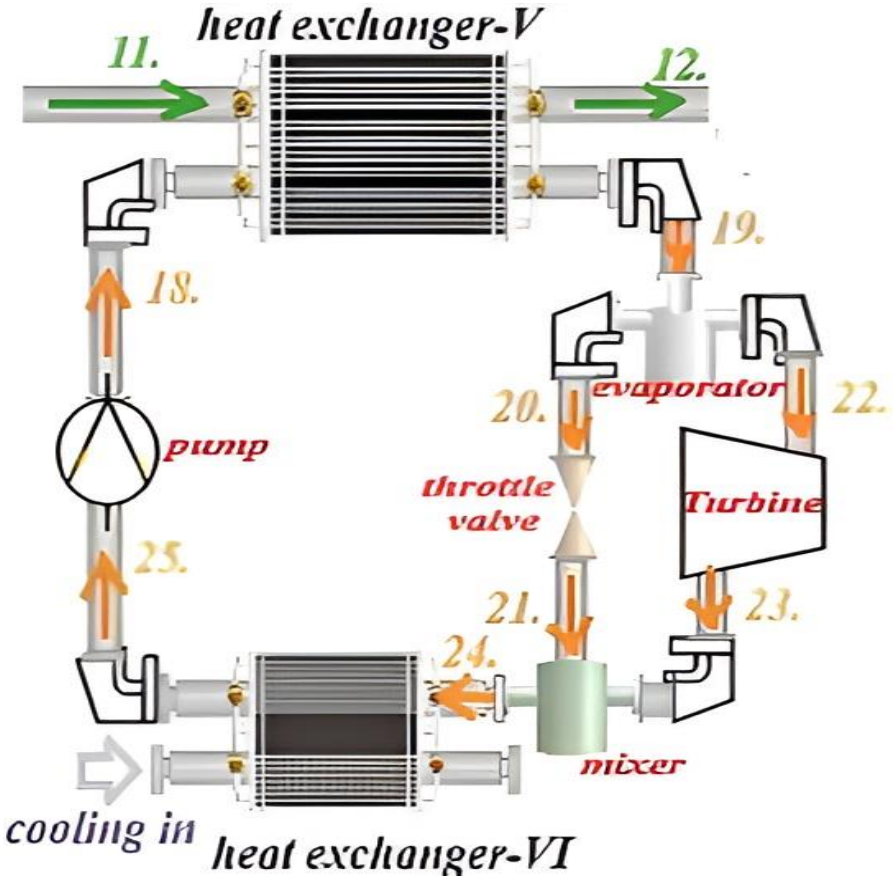

Figure 4. Kalina cycle flow chart.

Table 5. Thermodynamic properties of the cycle (T0. dead state).

Location	T [oC]	h [kJ/kg]	s [kJ/kg.K]	P [bar]	ex [kj/kg]	m [kg/s]	X [%NH_3]	Fluid
22.	115	1488	4.457	30	245	0.007204	0.9701	NH_3H_2O
23.	34.46	1267	4.585	5	-13	0.007204	0.9701	NH_3H_2O
20.	115	291.8	1.436	30	-82	0.000415	0.495	NH_3H_2O
21.	59.48	291.8	1.526	5	-107	0.000415	0.495	NH_3H_2O
24.	42.11	1164	4.267	5	-25	0.007618	0.92	NH_3H_2O
25.	40	130.8	0.6384	5	-13	0.007618	0.92	NH_3H_2O
18.	40.73	134.8	0.6433	30	-10	0.007618	0.92	NH_3H_2O
19.	115	1362	4.138	30	211	0.007618	0.92	NH_3H_2O
T[0].	25	-207.5	-0.5807	1	0	-------	----	NH_3H_2O

Table 6. Results obtained in the context of kalina.

Parameters	Values
Electric power ($\dot{W}_{kalina}$)	1.59 kW
Kalina heat transfer rate with heat exchanger-V ($\dot{Q}_{kalina}$)	9.35 kW
Kalina energy efficiency (η kalina)	16.9 %
Kalina exergy efficiency (ψ kalina)	10.9 %
exergetic sustainability index	0.20
Carbon emission	0.79 kg/h
Economic value of the electricity produced	7.74 $/h

Results obtained for Table 6 in the Kalina cycle are as follows: Electric Power for the Kalina cycle ($\dot{W}_{kalina}$): 1.59 kW. This value represents the electric power generated by the Kalina cycle. Kalina Heat Transfer Rate with Heat Exchanger-V ($\dot{Q}_{kalina}$): 9.35 kW. It signifies the heat flow rate transferred through heat exchanger-V in the Kalina cycle. Kalina Energy Efficiency (η_kalina): 16.9%. This value expresses the energy efficiency of the Kalina cycle, indicating how effectively it converts incoming energy into electrical energy. Kalina Exergy Efficiency (ψ_kalina): 10.9%. Exergy, a thermodynamic concept measuring the quality and usability of energy, indicates how efficiently the Kalina cycle utilizes energy resources. Exergetic Sustainability Index: 0.20.

This index evaluates the sustainability impact of the Kalina cycle. A low value may indicate less efficient use of energy resources or potentially more environmental harm. Carbon Emissions: 0.79 kg/h. Measuring the environmental impact, it represents 0.79 kg of carbon emissions per hour for the Kalina cycle. Produced Electric Economic Value: 7.74 $/h. This value denotes the economic performance of electricity generated by the Kalina cycle per hour. These results provide crucial information for the assessment of the Kalina cycle's energy conversion efficiency, sustainability index, and economic performance.

3.4. Findings Related To S-CO_2 And Kalina Cycles

The inclusion of Super Critical Carbon Dioxide (S-CO_2) and Kalina cycles in the system integration has significantly increased the power increase. In this context, a power

increase of 3.59 kW and an efficiency increase of 1.90% have been achieved in the system. These findings show that the system has a significant impact on its overall performance.

Power Increase and Efficiency Increase: The integration of S-CO_2 and Kalina cycles has contributed to the increase in total power by increasing energy production. The obtained increase of 3.59 kW shows a significant improvement in the total power of the system, while the efficiency increase of 1.90% increases the energy conversion efficiency.

Energy and Exergy Efficiency: At this point, the improvements in energy and exergy efficiencies achieved with the addition of S-CO_2 and Kalina cycles should be clearly demonstrated. S-CO_2 Cycle: The energy efficiency of the S-CO_2 cycle is determined as 15.9% and the exergy efficiency as 47.2%. This helps to minimize energy losses in the system. Kalina Cycle: The energy efficiency of the Kalina cycle is 16.9% and the exergy efficiency is 10.9%. The integration of the Kalina cycle provides an effective method for the recovery of low-temperature waste heat.

As a result, the inclusion of the S-CO_2 and Kalina cycles positively affected the overall performance by increasing the energy efficiency of the system. These findings provide the basis for further optimization of the system in future studies.

3.5. Result For Hot Water Analysis

Figure 5 shows the flow chart for the system used to obtain hot water.

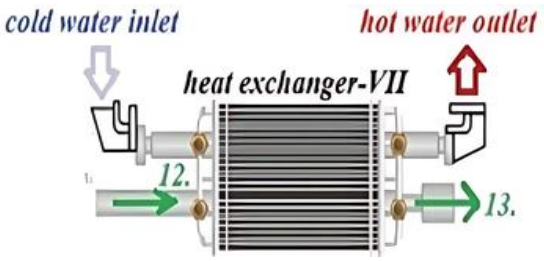

Figure 5. Hot water cycle flow chart.

Table 7. Thermodynamic properties of the cycle (T0. dead state).

Loc.	T [^{0}C]	s[kJ/ kg.K]	P [bar]	h [kJ/ kg]	ex [kj/ kg]	m [kg/s]
Cold water	25	0.3676	1	105.1	0	0.03588
Hot water	50	0.7043	1	209.6	4.108	0.03588
T0. water	25	0.3676	1	105.1	-----	------

Table 7 presents the thermodynamic properties of the cycle, focusing on the properties of cold water, hot water, and the reference water temperature. It provides information such as temperature (T), entropy (s), pressure (P), enthalpy (h), exergy (ex), and mass flow rate (m) for each type of water at different locations within the cycle. These properties are crucial for understanding the heat transfer and energy exchange processes occurring within the cycle.

Table 8. Results obtained in the hot water cycle.

Parameters	Values
Heat exchanger-VII heat flow rate	3.75 kW
Obtained useful heat flow rate	3.75 kW
Hot water energy efficiency (η water)	100 %
Hot water exergy efficiency (ψ water)	97 %
Carbon emission	1.875 kg/h

The results for the hot water cycle are presented in Table 8, offering insights into the energy conversion efficiency, exergetic efficiency, and environmental impact of Heat Exchanger-VII used for hot water production. High energy and exergetic efficiency, coupled with low carbon emissions, indicate the effective operation of the system in hot water generation.

3.6. Findings And Analysis Results Of The Integrated System

Table 9. Results Obtained from the Integrated System.

Parameters	Values
Energy analysis (SOFC+S-CO_2+kalina+water)	89.1 %
Exergy analysis (SOFC+S-CO_2+kalina+water)	64.6 %
Exergetic sustainability index (SOFC+S-CO_2+kalina)	0.83
Carbon emission (SOFC+S-CO_2+kalina+hot water)	98.06 kg/h

Table 9 shows that when the whole system is combined and an integrated system;

Energy Analysis (89.1%), When the integrated system includes SOFC, S-CO_2, Kalina cycle and hot water integration, the total energy analysis was measured at 89.1%. Compared to other studies, especially Hasanzadeh et al. [27] and You et al. Similar to [28] studies, this system has achieved a very high energy efficiency of 89.1%. This indicates that the energy in the integrated system is used effectively.

Exergy Analysis (64.6%), When the integrated system was evaluated with the integration of SOFC, S-CO_2, Kalina cycle and hot water, the exergy analysis results were determined as 64.6%. Gholamian et al. [29] study reported an exergy efficiency of 62.35% in an ORC-based system, which is similar to 64.6% in this study. This indicates that the energy in the system is used effectively in terms of exergy.

Exergetic Sustainability Index (0.83), The sustainability index is used to evaluate the sustainability of the integrated system including SOFC, S-CO_2 and Kalina cycles. In this study, the exergetic sustainability index value was determined as 0.83. This shows that energy integration is successful in terms of sustainability.

Carbon Emission (98.06 kg/h), Evaluated together with SOFC, S-CO_2, Kalina cycle and hot water integration, the integrated system produces 98.06 kg carbon emissions per hour. This is considered an important indicator for assessing environmental impact.

Produced Electricity Economic (33.85 $/h), The electricity economic value refers to the hourly electricity production economy of the integrated system including SOFC, S-CO_2 and Kalina cycles, and this value is determined as 33.85 $. A low electricity economy indicates an economically efficient energy integration.

Each cycle in the proposed system integration (SOFC, S-CO_2 and Kalina cycles) is compared with experimental studies in the existing literature. These comparisons are important in supporting the accuracy of the system's performance and are presented as follows:

SOFC (Solid Oxide Fuel Cell) Comparison: Experimental studies on SOFC in the literature show that these cells operate at high temperatures and provide high

energy efficiency. The SOFC in the proposed system provides 87.63% energy efficiency and 61.33% exergy efficiency, which is consistent with similar experimental studies in the literature. These data are consistent with the thermal management and energy conversion capability of the SOFC and the data in the literature.

S-CO_2 Cycle Comparison: Experimental studies on the S-CO2 cycle reveal that this system is an energy cycle that provides high efficiency and produces low carbon emissions. The 15.9% energy efficiency and 47.2% exergy efficiency obtained in our study are consistent with the experimental results in the literature and emphasize the environmental sustainability of the system.

Kalina Cycle Comparison: Experimental studies on the Kalina cycle in the literature show that this system is quite effective for the recovery of low-temperature waste heat. The 16.9% energy efficiency and 10.9% exergy efficiency obtained in the Kalina cycle in our study are consistent with similar experimental studies. These findings support that the Kalina cycle plays an effective role in the recovery of waste heat in our system. These comparisons confirm the accuracy of the performance of the proposed system integration and show that it largely overlaps with the experimental studies in the literature. However, the points where some aspects of the system differ from the experimental studies in the literature can be discussed and the reasons for these differences can be examined in future studies. Thermodynamic analyses were performed using the EES (Engineering Equation Solver) software [30].

4. Conclusion

The integration system shows high performance with its components including Solid Oxide Fuel Cell (SOFC), Super Critical Carbon Dioxide (S-CO_2) cycle, Kalina cycle and hot water recovery. While SOFC provides very successful results in terms of energy conversion efficiency, S-CO_2 and Kalina cycles have also been effective in electricity generation. Detailed energy and exergy analyses show that the existing energy resources in the system are used efficiently and that the system exhibits a sustainable profile with low carbon emissions.

• Energy and Exergy Efficiency: Detailed energy and exergy analyses show that the existing energy resources in the system are used efficiently and that it offers a sustainable profile with low carbon emissions.

• Exergy Analysis Results: Exergy analyses have determined the points where energy losses are the highest in the system. Optimizing the thermal management of the SOFC and efficient use of the ammonia-water mixture in the Kalina cycle will increase the exergy efficiency of the system. These improvements will be effective in minimizing energy losses and increasing system efficiency.

• Entropy Production Amounts: Entropy production values indicate the regions where thermodynamic irreversibilities in the system are concentrated. Entropy production can be reduced with optimizations, especially in heat exchangers and pressurized operating conditions. In this way, higher efficiency can be achieved. • Evaluation of Irreversibility: Irreversibility in each component of the system is examined in detail with advanced exergy analysis. In particular, while examining the components of the SOFC, S-CO_2 and Kalina cycles, the energy efficiency of the SOFC was determined as 87.63%, exergy efficiency as 61.33% and carbon emissions as 94.4 kg/h. These results show the potential of minimizing the environmental impacts of the system. The energy efficiency of the S-CO_2 cycle was determined as 15.9%, exergy efficiency as 47.2% and carbon emissions as 1 kg/h. These data reflect the effectiveness of the S-CO_2 cycle in energy conversion. The energy efficiency of the Kalina cycle was measured as 16.9%, exergy efficiency as 10.9% and carbon emissions as 0.79 kg/h. These results show how the Kalina cycle uses energy resources.

• Areas for improvement: The energy efficiency of the SOFC is 87.63% and the exergy efficiency is 61.33%. These efficiency values indicate that the thermal management of the SOFC needs to be optimized. Improving the thermal management will reduce energy losses and increase the overall efficiency of the system. S-CO_2 Cycle: The energy efficiency of the S-CO_2 cycle is 15.9% and the exergy efficiency is 47.2% (Table 4). These values indicate that optimization of the heat exchangers and other components in the cycle is necessary. Improvements to the heat exchangers can increase the overall efficiency of the S-CO_2 cycle by increasing the heat transfer efficiency. Kalina Cycle: The energy efficiency of the Kalina cycle is 16.9% and the exergy efficiency is 10.9% (Table 6). More efficient use of the ammonia-water mixture in the Kalina cycle is critical to increasing the energy conversion efficiency. Optimization of the ammonia-water mixture can contribute to increasing exergy efficiency. Hot Water Recovery System: The results in Table 8 show that the energy efficiency of the hot water recovery system is 100% and the exergy efficiency is 97%. High efficiency values indicate the effectiveness of the hot water production system, while indicating that the current system can be improved with further integration and optimization. These findings are associated with suggestions for increasing the exergy efficiency of the system, defining applicable improvement areas. Thus, the overall efficiency of the system is increased, contributing to sustainable energy production. As a result, the integrated system approach presented in this study provides significant contributions in terms of energy efficiency and sustainability, and shows higher performance compared to current systems.

Nomenclature

Cei	Exergoenvironmental impact coefficient	-
COP	Coefficient of performance	-
E	Energy consumption	kW·h
eCO_2	Carbon intensity factor	$kgCO_2/kW·h$
ex	Exergy	kJ/kg
fei	Exergoenvironmental impact factor	-
h	Enthalpy	kJ/kg
HHV_{H2}	Higher heating value of hydrogen	kJ/kmol
m	Mass flow rate	kg/s
P	Pressure	Bar
s	Entropy	kJ/kg·K
T	Temperature	∘C
T_{fc}	Fuel cell absolute temperature	K
η	Efficiency	%
η_{fc}	Fuel cell energy efficiency	%
η_{Kalina}	Energy efficiency of Kalina cycle	%
η_{S-CO2}	Energy efficiency of S-CO_2 cycle	%
Φei	Exergoenvironmental impact index	-
Φest	Exergetic sustainability index	-
ψ	Exergy efficiency	%
ψ_{fc}	Fuel cell exergy efficiency	%
ψ_{Kalina}	Exergy efficiency of Kalina cycle	%
ψ_{S-CO2}	Exergy efficiency of S-CO_2 cycle	%
$\dot{N}$	Molar flow rate	kmol/s

$\dot{Q}$	Heat transfer rate kW	
$\dot{S}_g$	Entropy generation rate	kW/K
$\dot{W}$	Electric power kW	
Δh	Change in enthalpy	kJ/kmol
Δs	Change in entropy	kJ/kmol·K

References:

[1] Y. Liu, J. Han, and H. You, "Exergoeconomic analysis and multi-objective optimization of a CCHP system based on SOFC/GT and transcritical CO_2 power/refrigeration cycles," *Appl. Therm. Eng.*, vol. 230, p. 120686, 2023.

[2] D. Wang, H. A. Dhahad, M. A. Ali, S. F. Almojil, A. I. Almohana, A. F. Alali, and K. T. Almoalimi, "Environmental/Economic assessment and multi-aspect optimization of a poly-generation system based on waste heat recovery of PEM fuel cells," *Appl. Therm. Eng.*, vol. 223, p. 119946, 2023.

[3] Y. Ji-chao and B. Sobhani, "Integration of biomass gasification with a supercritical CO_2 and Kalina cycles in a combined heating and power system: A thermodynamic and exergoeconomic analysis," *Energy*, vol. 222, p. 119980, 2021.

[4] Z. Wang, Y. Ma, M. Cao, Y. Jiang, Y. Ji, and F. Han, "Energy, exergy, exergoeconomic, environmental (4E) evaluation and multi-objective optimization of a novel SOFC-ICE-SCO2-HRSG hybrid system for power and heat generation," *Energy Convers. Manag.*, vol. 291, p. 117332, 2023.

[5] Y. Zhou, X. Han, D. Wang, Y. Sun, and X. Li, "Optimization and performance analysis of a near-zero emission SOFC hybrid system based on a supercritical CO2 cycle using solar energy," *Energy Convers. Manag.*, vol. 280, p. 116818, 2023.

[6] W. Liang, Z. Yu, F. Bian, H. Wu, K. Zhang, S. Ji, and B. Cui, "Techno-economic-environmental analysis and optimization of biomass-based SOFC poly-generation system," *Energy*, vol. 285, Art. no. 129410, Jan. 2023.

[7] H. R. Abbasi, H. Pourrahmani, and N. Chitgar, "Thermodynamic analysis of a tri-generation system using SOFC and HDH desalination unit," *Int. J. Hydrogen Energy*, vol. 46, no. 18, pp. 12345-12357, 2021.

[8] N. Chitgar, M. A. Emadi, A. Chitsaz, and M. A. Rosen, "Investigation of a novel multigeneration system driven by a SOFC for electricity and fresh water production," *Energy Convers. Manag.*, vol. 196, pp. 296–310, 2019.

[9] A. Kumar, A. K. Yadav, and S. Sinha, "Techno-Economic and Environmental Analysis of a Hybrid Power System formed from Solid Oxide Fuel Cell, Gas Turbine, and Organic Rankine Cycle," *J. Energy Resour. Technol.*, vol. 146, pp. 1–30, 2024.

[10] A. Arsalis and G. E. Georghiou, "A decentralized, hybrid photovoltaic-solid oxide fuel cell system for application to a commercial building," *Energies*, vol. 11, no. 12, p. 3512, 2018.

[11] P. Ran, X. Zhou, Y. Wang, Q. Fan, D. Xin, and Z. Li, "Thermodynamic and exergetic analysis of a novel multi-generation system based on SOFC, micro-gas turbine, S-CO2 and lithium bromide absorption refrigerator," *Appl. Therm. Eng.*, vol. 219, p. 119585, 2023.

[12] J. Pirkandi, M. Ghassemi, M. H. Hamedi, and R. Mohammadi, "Electrochemical and thermodynamic modeling of a CHP system using tubular solid oxide fuel cell (SOFC-CHP)," *J. Cleaner Prod.*, vol. 29, pp. 151–162, 2012.

[13] Y. Cao, S. Alsharif, E. A. Attia, M. A. Shamseldin, and B. F. Ibrahim, "A conceptual process design towards CO2 emission reduction by integration of solar-based hydrogen production and injection into biomass-derived solid oxide fuel cell," *Process Saf. Environ. Prot.*, vol. 164, pp. 164–176, 2022.

[14] U. Gunes, A. S. Karakurt, and B. Sahin, "The effect of size on entropy generation for waste heat recovery boiler," in *Proc. 32nd Int. Conf. Eff., Cost, Optim., Simul. Environ. Impact Energy Syst.*, 2019, pp. 809–818.

[15] E. Yücel, B. Doğanay, F. Gökalp, N. Baycık, and Y. Durmuşoğlu, "Kalina çevriminin bir tanker gemisine entegrasyonu ve geminin enerji verimliliğine etkisinin analizi," *Seatific*, vol. 1, no. 1, pp. 26–36, Dec. 2021.

[16] T. Koroglu and O. S. Sogut, "Advanced exergoeconomic analysis of organic rankine cycle waste heat recovery system of a marine power plant," *Int. J. Thermodyn.*, vol. 20, no. 3, pp. 140–151, 2017.

[17] Y. Ust, A. S. Karakurt, and U. Gunes, "Performance analysis of multipurpose refrigeration system (MRS) on fishing vessel," *Pol. Maritime Res.*, vol. 23, no. 2, pp. 48–56, 2016.

[18] J. Sieres and J. A. Martínez-Suárez, "Simulation of an integrated hydrogen fuel cell with LIBR-water absorption system for combined production of electricity, cooling and hot water," in *Proc. 8th Int. Conf. Heat Transfer, Fluid Mechanics, and Thermodynamics (HEFAT)*, Pointe Aux Piments, Mauritius, Jul. 2012, pp. 1163–1170.

[19] R. A. Gaggioli and W. R. Dunbar, "Emf, maximum power and efficiency of fuel cells," *Energy Resour. Technol.*, vol. 115, pp. 100–104, 1993.

[20] Y. A. Cengel and M. A. Boles, *Thermodynamics: An Engineering Approach*, 8th ed. New York, NY, USA: McGraw-Hill, 2011.

[21] I. Dincer and M. A. Rosen, *Exergy: Energy, Environment and Sustainable Development*, 2nd ed. Amsterdam, The Netherlands: Elsevier Science, 2012.

[22] A. Bejan, G. Tsatsaronis, and M. Moran, *Thermal Design and Optimization*. New York, NY, USA: John Wiley & Sons, 1996.

[23] M. Sharifishourabi, "Energetic and Exergetic Analysis of a Solar Organic Rankine Cycle with Triple Effect Absorption System," M.S. thesis, Eastern Mediterranean Univ. (EMU), Famagusta, Cyprus, 2016.

[24] J. Jeswiet and S. Kara, "Carbon emissions and CES™ in manufacturing," *CIRP Annals*, vol. 57, no. 1, pp. 17–20, 2008.

[25] International Energy Agency (IEA), "Global Energy & CO_2 Data," 2018. [Online]. Available: https://www.iea.org/countries. [Accessed: Aug. 2023].

[26] IRENA, "REmap 2030 commodity prices," [Online]. Available: https://www.irena.org/-media/Files/IRENA/REmap/Methodology/IRENA_REmap_2030_commodity_prices.xlsx?la=en&hash=505B546E4EE80A557363781E83EA1AE83D9FB256. [Accessed: Aug. 2023].

[27] A. Hasanzadeh, A. Chitsaz, P. Mojaver, and A. Ghasemi, "Stand-alone gas turbine and hybrid MCFC and SOFC-gas turbine systems: Comparative life cycle cost, environmental, and energy assessments," *Energy Rep.*, vol. 7, pp. 4659–4680, 2021.

[28] H. You, Y. Xiao, J. Han, A. Lysyakov, and D. Chen, "Thermodynamic, exergoeconomic and exergoenvironmental analyses and optimization of a solid oxide fuel cell-based trigeneration system," *Int. J. Hydrogen Energy*, vol. 48, no. 11, pp. 15950–15965, 2023.

[29] E. Gholamian and V. Zare, "A comparative thermodynamic investigation with environmental analysis of SOFC waste heat to power conversion employing Kalina and Organic Rankine Cycles," *Energy Convers. Manag.*, vol. 117, pp. 150–161, 2016.

[30] S. A. Klein, *Engineering Equation Solver (EES)*, F-Chart Software, Version 10.835-3D, 2020.